Coherent transport of atomic wave packets in amplitude-modulated vertical optical lattices

A. Alberti, G. Ferrari, V. V. Ivanov, M. L. Chiofalo*, and G. M. Tino†

Dipartimento di Fisica and LENS - Università di Firenze, CNR-INFM, INFN - Sezione di Firenze, via Sansone 1, 50019 Sesto Fiorentino, Italy

We report on the realization of dynamical control of transport for ultra-cold ^{88}Sr atoms loaded in an accelerated and amplitude-modulated 1D optical lattice. We tailor the energy dispersion of traveling wave packets and reversibly switch between Wannier-Stark localization and driven transport based on coherent tunneling. Within a Loschmidt-echo scheme where the atomic group velocities are reversed at once, we demonstrate a novel mirror for matter waves working independently of the momentum state and discuss possible applications to force measurements at micrometric scales.

PACS numbers: 03.75.Lm, 37.10.Jk, 03.65.Yz, 04.80.-y

Atoms trapped in optical lattice potentials in the absence of defects and phonon excitations, are extremely versatile systems for quantum applications [1] including transport [2] and strongly correlated phases [3]. In addition, control of atomic interactions may keep the dynamics coherent over seconds [4], and has led to atomic optical clocks with extraordinary performances [5], determination of forces at micrometer resolution [4, 6, 7, 8], and quantum information processing [9].

Tailoring and control of the coherent transport behavior is an essential tool for these applications [10]. Dynamical mechanisms, such as phase or amplitude lattice modulations, can be designed to drive trasport behavior over desired time and length scales. Phase modulation, obtained by a periodic spatial displacement of the optical lattice, has been earlier exploited to investigate quantum chaos [11] and, under the effect of constant forces, to observe Wannier-Stark resonances [12], photon-assisted resonant tunneling [13], quantum transport over macroscopic distances [14], and dynamical control of Mott insulator transitions [15]. Amplitude driving has been used so far as a spectroscopic tool for interband excitations [16], and to characterize the Mott insulator regime [17]. Analogous techniques are produced by acoustoelectric means in semiconductors nanostructures in the form of surface acoustic waves [18], but in this case the relevant spatial scale is much longer than the underlying static lattice.

In this Letter we report on dynamical control of coherent transport of quantum wave packets which is realized through amplitude modulation of vertical optical lattices. The control of transport allows to reverse all the atomic velocities at once, as in an atom mirror, assessing an effect similar to Loschmidt echos [19], and it provides a new tool for precise force measurements with micrometric spatial resolution. While extensive theoretical studies on phase-modulation of optical lattices are available [20, 21, 22], the physics underlying the control of transport through amplitude modulation is to our knowledge largely unexplored.

In the experiment, a 1D optical lattice for ^{88}Sr atoms is originated by the interference pattern of two vertical counter-propagating laser beams with wavelength λ_L, so that atoms effectively see a periodic potential with a period $d = \lambda_L/2$ and a depth dictated by the laser intensity, which we modulate in time. Our system is then described by the 1D time-dependent single-particle Hamiltonian:

$$\mathcal{H}(z,p,t) = \frac{p^2}{2m} - U(z)\left[1+\alpha f(t)\right] + mgz \qquad (1)$$

where $U(z) = U_0\cos(2k_Lz)/2$ and $f(t) \equiv \sin\big[\omega_M(t-t_0)-\phi\big]$. As in Fig. 1a, U_0 is the lattice depth, $k_L = 2\pi/\lambda_L$ is the laser wave vector, m is the atomic mass, g is the gravity acceleration along the lattice direction, $0 < \alpha < 1$ is the modulation amplitude expressed in units of U_0, $\omega_M = \ell\omega_B$ is the ℓ–th harmonic of the Bloch frequency $\omega_B = mgd/\hbar$, and t_0 the time when the modulation is switched on with initial phase ϕ. When $\alpha = 0$, the resulting static Hamiltonian $\mathcal{H}_0$ is diagonalized by the so-called Wannier-Stark states $\big|n\rangle$ centered at the n–th lattice site and separated in energy by quanta of $\hbar\omega_B$. In these conditions, wave packet tunneling is frozen due to Wannier-Stark localization and Bloch oscillations occur [2], where the quasi-momentum spans the Brillouin zone $[-k_L, k_L]$ with period $\tau_B = 2\pi/\omega_B$.

When the modulation is on at frequency $\ell\omega_B$ a coherent resonant tunneling is established between sites spatially separated by ℓd [13], as sketched in Fig. 1a. In the rotating wave approximation, the application of the unitary transformation $\mathcal{U} = \exp(-i\mathcal{H}_0t)$ simplifies the Hamiltonian of Eq. (1) into $\mathcal{H}' = \sum_{n=-\infty}^{\infty}\big[i(\mathcal{J}_\ell/2)e^{i\phi}\big|n+\ell\rangle\langle n\big| + \text{h.c.}\big]$ with tunneling rates $\mathcal{J}_\ell = -\alpha U_0\langle n+\ell\big|\cos(2k_Lx)\big|n\rangle/2$ [23]. This site-to-site tunneling can be equivalently viewed as a two-photon stimulated Raman process induced by the electric field of the lattice laser which acquires sidebands displaced by $\ell\omega_B$ [16], and it offers an alternative approach to [8]. In this pictures the $\mathcal{J}_\ell$ coefficients play the role of Frank-Condon factors [24]. In the momentum space, the

*Permanent address: Department of Mathematics and INFN, University of Pisa, Largo B. Pontecorvo 5, 56127 Pisa, Italy

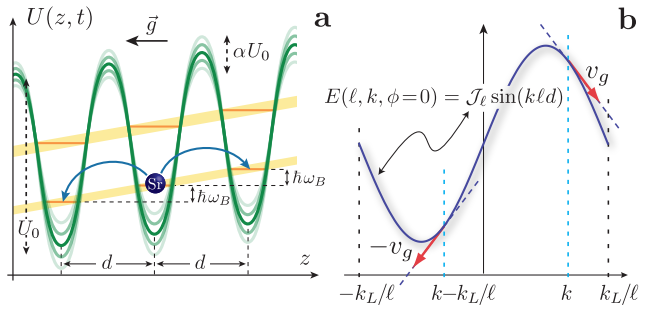

FIG. 1. Sketch of the transport mechanism in the amplitude-modulated (AM) lattice. (a) In the real space: Wannier-Stark localized states populate the tilted lattice of energy potential $U(z,t)$. In the absence of AM, $\alpha = 0$, the intersite tunneling is suppressed. Coherent tunneling between sites ℓd apart is enabled when AM is switched on at $\omega_M = \ell\omega_B$. (b) In the momentum space: wave packets behave as if they were moving in an effective sinusoidal energy band, whose width, periodicity and phase can be tailored by means of the AM parameters. Because of the sinusoidal shape, the group velocity v_g is reversed when $k \to k - k_L/\ell$.

atomic wave packets behave as if they were moving with an effective energy dispersion:

$$E(\ell, k, \phi) = \mathcal{J}_\ell \sin(k\ell d - \phi) \qquad (2)$$

as depicted in Fig. 1b, where each of the three parameters $\mathcal{J}_\ell$, ℓ and ϕ can be accurately tuned. This tunable sinusoidal energy profile has deep consequences for the trasport behavior. First, the size of the Brillouin zone is effectively reduced by a factor ℓ. Contrary to the subwavelength lattice studied in [25, 26], this is equivalent to establish an effective super-lattice period ℓd where the modulation at the ℓ–harmonics of ω_B controls the addressing of the ℓ–th site. Second, both ϕ and the energy bandwidth $\mathcal{J}_\ell$ can be tuned, the latter being linear in the full range of modulation amplitudes $0 < \alpha < 1$. Finally, the group velocity $v_g(\ell, k, \phi) = \partial E(\ell, k, \phi)/\partial(\hbar k) = \ell d \mathcal{J}_\ell \cos[k\ell d - \phi]/\hbar$ reverses its sign whenever $k \to k + (2n+1)\, k_L/\ell$ for any integer n, as shown in Fig. 1b. This recalls the Loschmidt-echo scheme in [19], where it is shown that the wave vector mapping is equivalent to reversing the band curvature $\mathcal{J}_\ell \to -\mathcal{J}_\ell$. This reversal can be a powerful tool to study decoherence processes and fidelity in quantum many-body systems [27]. We thus proceed to illustrate the experiment where this velocity reversal is performed.

The source of ultra-cold atoms has been described elsewhere [4]. Shortly, we start by trapping and cooling about 2×10^7 ^{88}Sr atoms at 3 mK in a magneto-optical trap (MOT) operating on the $^1S_0 - {}^1P_1$ resonance transition at 461 nm. The temperature is further reduced by a second cooling stage in a red MOT operating on the $^1S_0 - {}^3P_1$ intercombination transition at 689 nm. Finally we obtain $\sim 1 \times 10^6$ atoms at 1 μK. We load the atoms in the optical lattice which is switched on adiabatically in 80 μs. The atomic sample arranges itself in a disk-shaped geometry with a vertical RMS size of about $\sigma_0 = 30$ μm. Atomic interactions here are negligible because of the tiny scattering length in the ground state $a = -1.4\, a_0$ [28]. The lattice potential is originated by a single-mode frequency-doubled Nd:YVO_4 laser ($\lambda_L = 532$ nm) delivering up to 1 W on the atoms with a beam waist of 250 μm. The beam is vertically aligned and retro-reflected by a mirror. The resulting Bloch frequency is $\omega_B = 2\pi \times 574.3$ s^{-1}. The corresponding photon recoil energy is $E_R = h^2/(2m\lambda_L^2) = 2\pi \times 8000$ s^{-1}, and lattice depth ranges from 5 to 20 E_R, when the energy gap at k_L is $E_G \gtrsim 3\, E_R \gg \hbar\omega_B$ and the bandwidth is always smaller than $10^{-1} E_G$. Given these conditions, Landau-Zener tunneling is negligible. By controlling the radio-frequency power of an acousto-optical modulator we stabilize and modulate the laser intensity in order to reproduce the time-dependent Hamiltonian in Eq. 1. The readout is performed by measuring *in situ* the spatial atomic distribution using resonant absorption imaging.

To characterize the tunneling rates $\mathcal{J}_\ell$ we proceed as follows. The atoms are initially loaded in single lattice sites, their quasi momenta being spread over the whole Brillouin zone. In fact, the de Broglie wavelength results $\lambda_{\rm dB} \sim 200\,{\rm nm} < d$ at temperature $T \sim 1\,\mu$K. Applying the amplitude modulation for a given time results into a spatial broadening of the atomic wave packets. The speed of this broadening corresponds to the average over k of the group velocities $\langle v_g^2 \rangle^{1/2} = \ell d \mathcal{J}_\ell/(\sqrt{2}\hbar)$ which, thus, provides a measurement of $\mathcal{J}_\ell$. We measure the speed of broadening varying the modulation amplitude $0 < \alpha < 1$, and find that the $\mathcal{J}_\ell$ depend linearly on it. This is a unique feature of amplitude modulation which provides a clean tunability of the $\mathcal{J}_\ell$ in a wide range. As a function of U_0 and ℓ, we observe that the tunneling rates are well fitted by $|\mathcal{J}_\ell(U_0/E_R)| \approx |\mathcal{J}_1(U_0/E_R)| \exp[-\beta_1 (\ell - 1) U_0/E_R]$ with $\beta_1 = 0.35$ and $|\mathcal{J}_1(U_0/E_R)|/\hbar \approx 2500 \times (\alpha U_0/E_R) \exp(-\beta_2\, U_0/E_R)\, {\rm s}^{-1}$ with $\beta_2 = 0.25$. This agrees with the expression which can be calculated employing the Wannier-Stark basis.

In order to demonstrate the reversal of the group velocities, we employ the sequence in Fig. 2a, using a Loschmidt-echo scheme analogous to the more familiar spin echo in other systems [19]. Two identical AM bursts at $\ell\omega_B$ are applied lasting $287\,\tau_B \sim 500$ ms each, where τ_B has been preliminarily measured with 1 ppm sensitivity [13]. For each case $\ell = 1, 2, 3$, $U_0 = 11.2,\ 6.6,\ 6.3\ E_R$ and $\alpha = 0.23, 0.47, 0.84$ are chosen to keep comparable tunneling rates. The two bursts serve to enable the coherent tunneling and are separated by a variable *freezing time* $t_{\rm fr}$ (with $t_0 = 0$ and $\phi = 0$), during which AM is off and tunneling is disabled. During the *freezing time*, Bloch oscillations occur in the reduced Brillouin zone $[-k_L/\ell, k_L/\ell]$ which is spanned by the atomic wave vector k with an effective Bloch period $\tau_\ell = \tau_B/\ell$. The magnitude and sign of $v_g(\ell, k, \phi)$ change while k spans the Brillouin zone, so that the atomic cloud is expected to expand or shrink de-

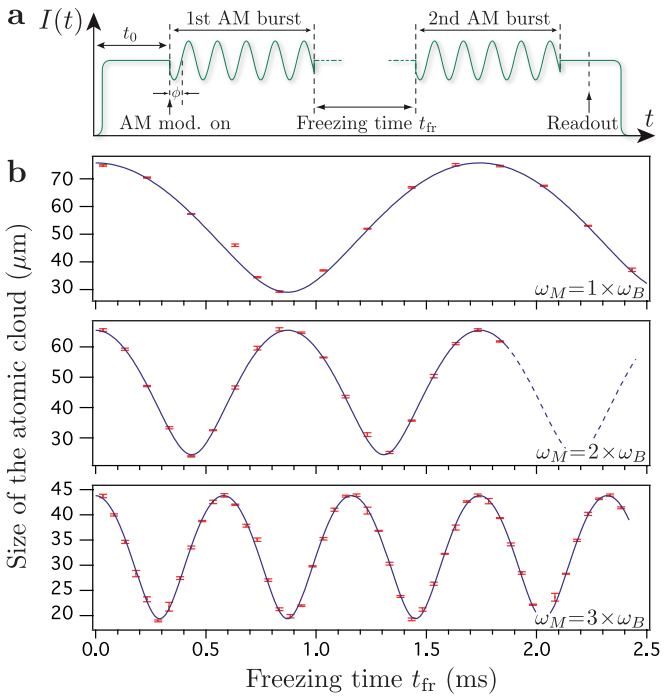

FIG. 2. Realization of Loschmidt echos (a) The applied sequence: two identical AM bursts of the optical lattice intensity $I(t)$ at $\ell\omega_B$ enable the resonant tunneling which couples lattice sites separated by ℓd. The bursts are separated by a *freezing time* $t_{\rm fr}$, during which the tunneling is disabled and Bloch oscillations of the quasi momentum set in. (b) The corresponding cloud's RMS size *vs.* $t_{\rm fr}$ has periodicity $2\pi/(\ell\omega_B)$. From top to bottom, AM at $\omega_M = \ell\omega_B$ induces resonant coupling with up to $\ell = 3$ neighboring sites. Inversion of the group velocities v_g occurs at the minima of the RMS size.

pending on the value of v_g reached at the start of the second burst. Fig. 2b shows that this is indeed the case, resulting in a periodic signal with period τ_ℓ. The group velocities $v_g(\ell, k, \phi)$ are fully reversed independently of the k values at each $\tau_\ell/2$, that is at the minima occurring at $t_{\rm fr} = \tau_\ell/2|2n+1|$ (n integer). The Gaussian convolution of the single atom response with the initial cloud's distribution suggests that the expression of the RMS size is $\sigma(t_{\rm fr}) = \sqrt{\sigma_0^2 + \sigma_1^2\cos(\pi\, t_{\rm fr}/\tau_\ell)^2}$, with σ_0 the initial size. This is reproduced by the solid curves, best agreeing with the measured points. The fit to each data set with different ℓ yields $\tau_\ell = \tau_B/\ell$, and σ_1 turns out to match the broadening which would occur after one single burst twice as long. The oscillations persist undamped over several seconds, indicating a high fidelity in recovering the quantum state after v_g reversal [19].

In order to observe the mirror effect for traveling matter waves with defined momentum, we need to prepare the atoms with a momentum dispersion narrower than the Brillouin zone. We accomplish this by increasing $U_0 = 14\ E_R$ sufficiently to trap a fraction of atoms also in the second band, where the momentum distribution shrinks since here the thermal momentum distribution is steeper. In addition, we purposely favor one of the two directions by letting the atoms freely fall for about 200 μs between the release from the red MOT and the lattice switch on. We can accurately control the value of k within the Brillouin zone by following the Bloch oscillations in the static lattice for a time t_0 before activating the amplitude modulation. During the modulation the cloud's position is expected to move with a velocity $v_g(\ell, k, \phi)$ with $k = k_L t_0/\tau_B$, as it is shown in Fig. 3 . At the flex points of $E(\ell, k, \phi)$, like at $k = 0$ for $\phi = 0$, the motion becomes dispersionless and reaches the largest v_g, and consequently the largest displacement. In this case, Fig. 4 shows the displacement of the atoms in the second band which move upwards with a v_g of 0.64 mm/s when $\alpha = 0.33$ and $\ell = 1$. We track this motion for 500 cycles on a distance of about 0.5 mm. A residual broadening still occurs because of finite spread of the initial momentum distribution, but it is limited to 1/10 of the total displacement. This can be largely reduced by initially preparing a narrower momentum distribution, as with Bragg or Raman velocity selective stages, sympathetic cooling or BECs. In order to reverse the wave-packets' motion we subsequently apply the scheme of Fig. 2a by choosing $t_{\rm fr} = \tau_B/2$. During the second burst the atoms move downwards with the same speed but opposite direction. As expected, the atom mirror reverses the direction of motion as well as the broadening of the atomic cloud, making the traveling wave packets recover their initial size after 500 cycles of the second burst.

Tailoring the transport with AM in a lattice could provide an excellent tool in the study of potentials at short distances from a surface, e.g. the Casimir-Polder interaction, since it allows to measure forces with micrometric spatial resolution and high sensitivity. For instance, we report a measurement of g with relative sensitivity *e.g.* $\Delta g/g = 5\times10^{-7}$, which is obtained following the

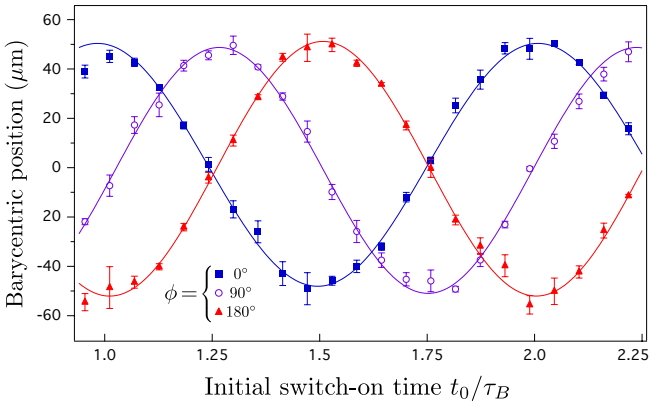

FIG. 3. Cloud's barycentric position after a single AM burst *vs.* swtich-on time of the AM modulation, t_0, at $\omega_M = \omega_B$. By varying the modulation phase ϕ of the driving we shift the sinusoidal dispersion law by the same amount, *e.g.* at $\phi = 90°$ from sine to cosine.

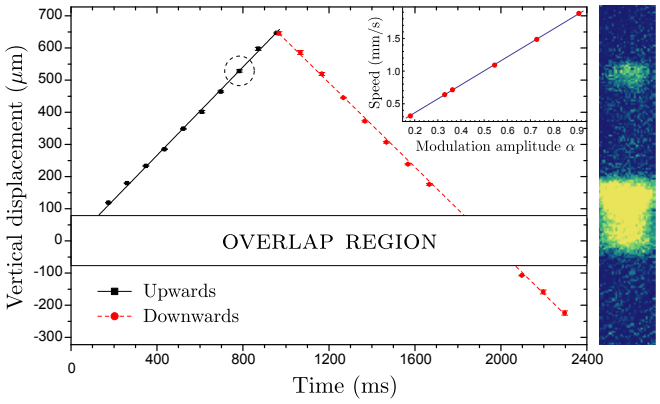

FIG. 4. Atom mirror for traveling matter waves. Atoms loaded in the 2nd band have sub-recoil momentum dispersion. Wave packets with initial $k = 0$ travel upwards with minor dispersion (solid line). After reversing the group velocity v_g, atoms move downwards with opposite speed (dashed line). Inset: linearity of the tunneling *vs* the modulation amplitude α. Right panel: 2D density profile of the cloud corresponding to the data point, circled in figure, at $t = 783$ ms. Since the atoms in the 2nd band have an higher v_g, the two clouds separate each other away from the origin.

oscillations in Fig. 2b at $\omega_M = 3\omega_B$ for 7 seconds. The amplitude modulation method can also be employed in a single pulse scheme as in [13] for phase modulation, with the significant advantage that now it can be implemented in the vicinity of a reflective substrate since an independent control of the two lattice beams is not required. In addition, compared to other methods based on the study of Bloch oscillations in static lattices [7, 29], our method has the advantage of being insensitive to the temperature of the atomic sample, and being suited to measure potential profiles even with strong curvature.

In conclusion, we presented a novel method to tailor the transport of cold atoms in optical lattices. By modulating the intensity of the lattice we are able to modify the fundamental properties governing the transport such as the dimension of the Brillouin zone and the width of the sinusoidal energy band. This allows us to realize a Loschmidt-echo scheme, offering a new tool for the study of decoherence phenomena as well as for applications in atom optics. Force measurements with sub-ppm sensitivity and micrometric spatial resolution were obtained, suggesting additional applications in the field of force measurements at short distances from a surface.

We thank M. Artoni for critical reading, M. Schioppo for experimental assistance, V. Piazza for helpful discussions, and R. Ballerini, M. De Pas, M. Giuntini, A. Hajeb, A. Montori for technical assistance. This work was supported by LENS, INFN, EU (under contract RII3-CT-2003 506350 and FINAQS), ASI.

† Electronic address: guglielmo.tino@fi.infn.it

[1] I. Bloch, J. Dalibard, and W. Zwerger, Rev. Mod. Phys. **80**, 885 (2008).
[2] M. Raizen, C. Salomon, and Q. Niu, Physics Today **50**, 30 (1997).
[3] M. Greiner, O. Mandel, T. Esslinger, T. W. Hänsch, and I. Bloch, Nature **415**, 39 (2002).
[4] G. Ferrari, N. Poli, F. Sorrentino, and G. Tino, Phys. Rev. Lett. **97**, 060402 (2006).
[5] S. Blatt et al., Phys. Rev. Lett. **100**, 140801 (2008).
[6] B. P. Anderson and M. A. Kasevich, Science **282**, 1686 (1998).
[7] G. Roati E. de Mirandes, F. Ferlaino, H. Ott, G. Modugno, and M. Inguscio, Phys. Rev. Lett. **92**, 230402 (2004). I. Carusotto, L. Pitaevskii, S. Stringari, G. Modugno, and M. Inguscio, *ibid.* **95**, 093202 (2005).
[8] P. Wolf, P. Lemonde, A. Lambrecht, S. Bize, A. Landragin, and A. Clairon, Phys. Rev. A **75**, 063608 (2007).
[9] I. Bloch, Nature **453**, 1016 (2008).
[10] M. Grifoni and P. Hänggi, Phys. Rep. **304**, 229 (1998).
[11] W. K. Hensinger *et al.*, et al., Nature **412**, 52 (2001).
[12] S. R. Wilkinson, C. F. Bharucha, K. W. Madison, Q. Niu, and M. G. Raizen, Phys. Rev. Lett. **76**, 4512 (1996).
[13] V. V. Ivanov, A. Alberti, M. Schioppo, G. Ferrari, M. Artoni, M. L. Chiofalo, and G. M. Tino, Phys. Rev. Lett. **100**, 043602 (2008). C. Sias, H. Lignier, Y. P. Singh, A. Zenesini, D. Ciampini, O. Morsch, and E. Arimondo, *ibid.*, 040404 (2008).
[14] A. Alberti, V. V. Ivanov, G. M. Tino, and G. Ferrari, Nat. Phys. **5**, 547 (2009).
[15] A. Zenesini, H. Lignier, D. Ciampini, O. Morsch, and E. Arimondo, Phys. Rev. Lett. **102**, 100403 (2009).
[16] J. H. Denschlag, J. E. Simsarian, H. Häffner, C. McKenzie, A. Browaeys, D. Cho, K. Helmerson, S. Rolston, and W. D. Phillips, J. Phys. B **35**, 3095 (2002).
[17] T. Stöferle, H. Moritz, C. Schori, M. Köhl, and T. Esslinger, Phys. Rev. Lett. **92**, 130403 (2004).
[18] J. R. Gell and *et al.*, Appl. Phys. Lett. **93**, 081115 (2008).
[19] F. M. Cucchietti, D. A. Dalvit, J. P. Paz, and W. H. Zurek, Phys. Rev. Lett. **91**, 210403 (2003). F. M. Cucchietti, arXiv:quant-ph/0609202v1 (2006).
[20] D. H. Dunlap and V. M. Kenkre, Phys. Rev. B **34**, 3625 (1986).
[21] Q. Thommen, J. C. Garreau, and V. Zehnlé, Phys. Rev. A **65**, 053406 (2002).
[22] A. Eckardt, C. Weiss, and M. Holthaus, Phys. Rev. Lett. **95**, 260404 (2005).
[23] Since only resonant terms contribute to the tunneling, off-resonant interband transitions can be safely neglected, as well as Landau-Zener tunneling which is strongly suppressed in our experimental conditions.
[24] A. B. Deb, G. Smirne, R. M. Godun, and C. J. Foot, J. Phys. B **40**, 4131 (2007).
[25] W. Yi, A. J. Daley, G. Pupillo, and P. Zoller, New J. of Phys. **10**, 073015 (2008).
[26] T. Salger C. Geckeler, S. Kling, and M. M. Weitz, Phys. Rev. A **79**, 011605 (2009).
[27] W. H. Zurek, Rev. Mod. Phys. **75**, 715 (2003).
[28] Y. N. M. de Escobar *et al.*, Phys. Rev. A **78**, 062708 (2008).
[29] F. Sorrentino, A. Alberti, G. Ferrari, V. V. Ivanov, N. Poli, M. Schioppo, and G. M. Tino, Phys. Rev. A **79**, 013409 (2009).